치의학박사학위논문

Polymerization shrinkage strain, modulus, and shrinkage stress related to tooth-restoration interfacial debonding in bulk-fill composites

Bulk−fill 복합레진 수복시 치아−수복물 계면 파괴와 관련된 중합수축, 탄성계수, 수축응력

2015년 2월

서울대학교 대학원

치의과학과 치과보존학 전공

김 진 영

Abstract

Polymerization shrinkage strain, modulus, and shrinkage stress related to tooth-restoration interfacial debonding in bulk-fill composites

Ryan Jin-Young Kim, B.D.S., M.S.D.

Program in Conservative Dentistry

Department of Dental Science

Graduate School, Seoul National University

(Directed by Prof. In-Bog Lee, D.D.S., M.S.D., Ph.D.)

Objectives. The aim of the present study was to measure the polymerization shrinkage, modulus, and shrinkage stress of bulk-fill and conventional composites during polymerization and to investigate the relationship between tooth-composite interfacial debonding and polymerization shrinkage stress of the composites.

Methods. Polymerization shrinkage, dynamic modulus, and shrinkage stress of two non-

flowable bulk-fill: SonicFill (SF) and Tetric N-Ceram Bulk-Fill (TNB); two flowable bulk-fill: Filtek Bulk-Fill (FB) and SureFil SDR Flow (SDR); one non-flowable conventional: Filtek Z250 (Z250); and one flowable conventional: Filtek Z350 XT Flowable (Z350F) composites were measured using custom-made instruments. Acoustic emission (AE) analysis was performed to evaluate the tooth-composite interfacial debonding during polymerization of the composites in Class 1 cavities on extracted third molars.

Results. Polymerization shrinkage (%) of Z350F (3.53) at 10 min was the highest, followed by FB (3.05), SDR (2.99), TNB (2.22), Z250 (2.09), and SF (2.05). Complex shear modulus (MPa) after 20 s of light-curing was highest in SF (996.2), followed by Z250 (831.8), TNB (723.6), Z350F (553.2), SDR (421.3), and FB (334.8). Polymerization shrinkage stress values (MPa) were: Z350F (3.51), TNB (2.42), Z250 (2.38), SF (2.36), FB (2.24), and SDR (1.68). The numbers of AE events were: Z350F (12.6), TNB (7.0), Z250 (7.0), FB (6.8), SF (6.6), and SDR (6.0). Z350F showed the highest polymerization shrinkage stress and AE event number ($p < 0.05$). SDR exhibited the lowest polymerization shrinkage stress ($p < 0.05$). The polymerization shrinkage stress for TNB, Z250, SF, and FB as well as the number of AE events for TNB, Z250, FB, SF, and SDR were not significantly different ($p > 0.05$).

Conclusions. Composites that exhibited greater polymerization shrinkage stress generated more tooth-composite interfacial debonding. In contrast to similar outcomes among the non-flowable composites (conventional: Z250, bulk-fill: TNB and SF), the flowable bulk-fill composites (FB and SDR) demonstrated lower polymerization shrinkage stress and tooth-composite interfacial debonding than did the flowable conventional composite (Z350F).

Keywords: Acoustic emission, Bulk-fill composite, Modulus, Shrinkage, Stress

Student Number: 2012-31170

Contents

Abstract (in English)

1. Introduction …… 1

2. Materials and Methods …… 5

3. Results …… 12

4. Discussion …… 15

5. Conclusions …… 22

6. References …… 23

Table and Figures …… 29

Abstract (in Korean) …… 40

Polymerization shrinkage strain, modulus, and shrinkage stress related to tooth-restoration interfacial debonding in bulk-fill composites

Ryan Jin-Young Kim, B.D.S., M.S.D.

Program in Conservative Dentistry

Department of Dental Science

Graduate School, Seoul National University

(Directed by Prof. In-Bog Lee, D.D.S., M.S.D., Ph.D.)

1. Introduction

With the advancement of dental materials and clinical techniques, composites have become the most widely used direct restorative material to satisfy the patients' esthetic demand for the restoration of dental caries, crown fractures, tooth wear, and congenital defects.

A major drawback of composite is polymerization shrinkage, which reportedly occurs in the range of 2-5% during polymerization.[1-4] Polymerization shrinkage occurs as the distance between monomers is reduced when the weak van der Waals forces between monomers are converted into covalent bonds. Polymerization shrinkage generates stress at the tooth-restoration interface, resulting in de-bonding when the shrinkage stress surpasses the bond strength.[5] This, in turn, leads to a number of potential clinical problems such as post-operative hypersensitivity, secondary caries, and pulpal inflammation as a result of the penetration of saliva, bacteria, and other irritating substances through the debonded interface.

In order to minimize the stress from polymerization shrinkage, an incremental technique has been recommended,[6,7] in which the composite is placed and light-cured in increments of less than 2 mm. The incremental layering of composite reduces the C-factor, which is defined as the ratio of the bonded surface area to the unbonded surface area of the restoration.[8] This reduces the shrinkage stress at the tooth-composite interface by permitting the stress-relieving flow of composite from the unbonded surface to towards the bonded surface.

Recently, bulk-fill composites have been developed to simplify the rather time-consuming incremental procedure. Manufacturers claim that, opposed to conventional composites, bulk-fill composites can be placed in a single bulk layer because they generate

a lower polymerization shrinkage stress. In addition, bulk-fill composites have higher light transmission properties due to reduction of light scattering at the filler-matrix interface by either decreasing the filler amount or increasing the filler size.[9,10] In this way, bulk-filling to a depth of 4-5 mm is achievable without significantly impairing the degree of conversion.

According to viscosity, conventional and bulk-fill composites can be further classified into two types: non-flowable (high-viscosity) and flowable (low-viscosity) composites. Non-flowable composites (also known as paste or sculptable composites) are much more resistant to slumping and contain a greater amount of inorganic fillers. Flowable composites generally adapt better on the cavity wall, especially in irregular surfaces, and exhibit greater polymerization shrinkage and lower mechanical properties due to their lower filler contents. The inferior mechanical properties of flowable composites necessitate a 2-mm capping layer with a non-flowable composite when restoring areas subject to occlusal stress.[10]

Since the advent of bulk-fill dental composites, numerous studies have been published on bond strength,[11] cuspal deflection,[12] degree of conversion,[13] depth of cure,[9,14-17] internal and marginal adaptation,[18] mechanical properties,[9,10,13,17,19] microleakage,[12] shrinkage,[16] and shrinkage stress[20]. Despite the fact that manufactures claim that their bulk-fill composites have lower shrinkage stress, no studies have reported the debonding behavior of bulk-fill composites at the tooth-restoration interface compared to those of conventional

composites. Furthermore, the change in modulus of composites during polymerization plays a major role in the development of polymerization shrinkage stress; there is no study that has measured the development of the initial modulus of bulk-fill composites during polymerization.

The aim of the present study was to measure the polymerization shrinkage, dynamic modulus, and shrinkage stress of bulk-fill and conventional composites during polymerization and to investigate the relationship between tooth-composite interfacial debonding and polymerization shrinkage stress of composites. The null hypotheses of this study were: 1) there would be no differences in the polymerization characteristics, including polymerization shrinkage, modulus, and shrinkage stress, between the bulk-fill and conventional composites and 2) the tooth-composite interfacial debonding behavior is associated with shrinkage stress.

2. Materials and Methods

2.1. Materials

The name, type, composition, and manufacturer of the composites used in the present study are listed in Table 1. Four bulk-fill: two non-flowable (SonicFill, SF; Tetric N-Ceram Bulk Fill, TNB) and two flowable (SureFil SDR Flow, SDR; Filtek Bulk Fill, FB) composites were compared with two conventional: one non-flowable (Filtek Z250, Z250) and one flowable (Filtek Z350 XT Flowable, Z350F) composites in terms of shrinkage strain, modulus, shrinkage stress, and debonding behavior at the tooth-composite interface during polymerization. SonicFill was sonic activated (SonicFill handpiece, Kerr, Orange, CA, USA) to dispense the material, as recommended by the manufacturer. An LED light curing unit (Elipar S10 LED, 3M ESPE, St. Paul, MN, USA) with an irradiance of 750 mW/cm^2 was employed to light-cure the composites.

2.2. Measurement of axial polymerization shrinkage

A modified bonded disc method[21,22] was used to measure the axial polymerization shrinkage of the composite specimens (Fig. 1a). The instrument is comprised of a linear variable differential transformer (LVDT) probe (AX-1, Solartron Metrology, West Susssex,

UK) fixed on a vertical stage (Micro Motion Technology, Bucheon, Korea), equipped with a micrometer (Mitutoyo, Kawasaki, Japan) and a horizontal metal plate with a hole positioned under the LVDT probe.

A fixed amount of composite was pressed between a slide glass and a flexible cover glass (Marienfeld, Germany). A spacer consisting of a metal wire with a diameter of 0.5 mm was used to produce a 0.5-mm-thick specimen with a diameter of 6 mm. The specimen was positioned beneath the tip of the LVDT probe, which was then set to the zero point using the micrometer. The LVDT detected the axial linear shrinkage caused by polymerization.

For shrinkage measurements, the curing light (positioned 2 mm under the specimen) was turned on for 40 s after a 10 s baseline. The shrinkage values were stored on a computer using a data acquisition device (PCI-6024, National Instruments Co., Austin, Tx, USA) at a rate of 10 data points/s for 600 s. Five specimens were tested for each composite.

2.3. Measurement of the initial dynamic modulus of composites during curing

As in our previous studies,[21,23] a custom-designed oscillation rheometer was used to measure the initial viscoelastic dynamic modulus change of the composites during light-curing. The rheometer consists of three parts (Fig. 1b): (1) a measuring unit of parallel glass plates, between which the composite specimen was placed; (2) an oscillatory shear strain

induction unit with a DC motor and a crank mechanism; and (3) a stress-measuring unit using an electromagnetic torque sensor, composed of an electromagnetic actuator, a bi-cell photo diode (BCPD, SD 113-24-21-021, Advanced Photonix Inc., Camarillo, CA, USA), and a negative feedback servo amplifier.

For specimen preparation, the end faces of the parallel glass plates, which were made of a glass rod with a diameter of 3 mm, were sandblasted with 50-μm Al_2O_3 powder and treated with a silane coupling agent (Monobond S, Ivoclar Vivadent, Schaan, Liechtenstein). A certain volume (approximately 14 mm^3) of composite was placed into a 2-mm gap between the upper and lower glass rods of the measuring unit (parallel plate geometry). The light guide was positioned 2 mm from the sample.

A sinusoidal oscillating shear strain with an amplitude of 0.0091 at a frequency of 7 Hz was generated by the DC motor and crank mechanism and transmitted to the upper part of the measuring unit. The increase in the viscoelasticity of the composite sample during polymerization caused more shear force to be transmitted to the lower glass rod, as the upper rod of the measuring unit continuously oscillated. As a result, the arm of the torque sensor attached to the lower rod rotated from its null position, which changed the intensity of the infrared light from the LED to the BCPD. An electric voltage, generated by the BCPD, was fed to a servo amplifier. This allowed the current to flow into an actuator coil. Through this negative feedback mechanism, the arm of the torque sensor was always

maintained at the null position during the measurement, while the sensor measured the torque linearly without deviation. The driving current of the servo amplifier was proportional to the torque and was converted into a voltage and stored on a computer.

The initial modulus changes were recorded during 20 s of light-curing. The output signals from the potentiometer and the torque sensor were stored on a computer at a sampling rate of 1,000 points/s for 20 s using a data acquisition board (USB-6016, National Instruments Co., Austin, TX, USA) and custom-made software using LabVIEW 7.1 (National Instruments Co.). Five measurements were collected for each composite.

From the measured shear strain and torque, the complex shear modulus, G^* (Pa), was calculated using the following formula:

$$G^* = \frac{2TH}{\pi\omega R4},$$

where T is the measured torque amplitude (Nm), H is the distance between the two parallel plates (m), ω is the oscillation amplitude (rad), and R is the radius of the parallel plates (m).

2.4. Measurement of the polymerization shrinkage stress of composites

An instrument was manufactured to measure the polymerization shrinkage stress of composites during photo-polymerization (Fig. 1c).

One end face of each 1-mm-thick glass slide was sandblasted and covered with semi-transparent adhesive tape. After cutting a 4-mm-wide window in the center of the taped side of the glass slide, silane (Monobond S, Ivoclar Vivadent**)** was applied on the exposed sandblasted glass and air-dried. A thin layer of bonding agent (Adper Scotchbond Multi-Purpose Adhesive, 3M ESPE) was applied on the window and light-cured for 10 s. The glass slide was fixed to a stage mounted on a voice coil motor (MGV52-20-0.5, Akribis Systems, Singapore), and another glass slide was fixed to a stage on the opposite side of the voice coil motor. The two glass slides were fixed on the shrinkage-stress measuring instrument and were positioned 2 mm apart in series, with the windowed sides facing each other. The space between the windows (8 mm^3) was filled with one of the six composites. When the composite specimen shrank during polymerization, a linear encoder detected the micro-movement of the slide fixed to the voice coil motor as it was pulled toward the fixed slide on the left. In order to instantly eliminate deviation, the servo amplifier sent current proportional to the shrinkage force to the voice coil motor in order to maintain the original position of the glass slide fixed to the voice coil. The servo current was converted into a voltage, which was then stored on a computer via the data acquisition board.

For stress measurements, after obtaining a baseline for 10 s, the curing light (positioned 2 mm above the specimen) was turned on for 40 s. The polymerization shrinkage stress was recorded at a rate of 10 data points/s for 600 s. Each measurement was repeated five

times for each material

2.5. Acoustic emission (AE) analysis during composite curing

Thirty intact and caries-free extracted third molars were stored in a 0.5% chloramine-T solution. As in our previous study,[24] the roots were horizontally sectioned at 5 mm below the CEJ, and the pulp was removed carefully using tissue forceps and a file. The occlusal surface of the teeth was ground to a flat surface, and class I cavities (mesio-distal length, 5 mm; bucco-lingual width, 4 mm; depth, 3 mm; C-factor = 3.7) were created using a flat end cylindrical diamond bur. A 2-mm-diameter hole was made through the root in the mesio-distal direction so that the tooth could be attached to a glass slide with an elastic rubber band (Fig. 1d). Grease (Shin-Etsu Chemical Co. Ltd., Tokyo, Japan) was applied between the tooth and the glass slide. The cavities were etched with phosphoric acid (Etchant, 3M ESPE) for 15 s, rinsed with water, and then blotted dry. Primer (Adper Scotchbond Multi-Purpose Primer, 3M ESPE) and a bonding agent were then applied to the cavity walls and light-cured for 10 s.

An AE sensor (M204A, Rectuson, Sungnam, Korea) was attached to the glass slide with grease 1 cm from the tooth. After the cavity was filled with one of the six composites in bulk (60 mm^3), a 20 s baseline was obtained. Then, the composite was photo-polymerized from the occlusal surface for 40 s. The tip of the curing light was positioned 2 mm from

the specimen during this treatment. Following light-curing, the tooth was covered with wet gauze to prevent cracking from dehydration, which could lead to false signals. AE signals generated as a result of debonding at the tooth-composite interface were recorded for 2,000 s. The signals from the AE sensor were amplified (A1002, Rectuson) (2,500x) and stored on a computer using a data acquisition board (USB-6361, National Instruments Co.). The measurements were performed at a 2 MHz sampling rate, 2 ms duration, and 70 mV threshold.

2.6. Statistical analysis

The data were analyzed using one-way ANOVA followed by Tukey HSD post hoc comparison ($\alpha = 0.05$). Correlation analysis was performed to investigate the relationship between the stress and modulus, shrinkage, and AE events.

3. Results

3.1. Axial polymerization shrinkage

Representative curves of polymerization shrinkage (%) as a function of time for the six composites are presented in Fig. 2a.

In decreasing order, the shrinkage strains after 600 s were: Z350F 3.53 (0.09), FB 3.05 (0.05), SDR 2.99 (0.08), TNB 2.22 (0.06), Z250 2.09 (0.08), and SF 2.05 (0.05) (Fig. 2b). Shrinkage strains were similar among all of the non-flowable composites (conventional and bulk-fill), which demonstrated significantly less shrinkage than the flowable composites.

3.2. Initial dynamic modulus

The complex shear moduli (MPa) of composites during 20 s of light-curing are shown in Fig 3a. There were significant differences in the dynamic modulus (Fig. 3b) and the time (s) to reach a complex modulus (10 MPa and 100 MPa) (Fig. 3c) between the polymerizing composites. TNB showed the highest modulus at 5 s after light-curing, followed by SF, Z250, SDR, Z350F, and FB. However, at 20 s after light-curing, SF showed the highest modulus, followed by Z250, TNB, Z350F, SDR, and FB.

The time to reach the complex modulus of 10 MPa differed between materials, with SF and TNB being the fastest (2.2 s) and Z350F and FB being the slowest (4.7 s). The time to reach the complex modulus of 100 MPa was fastest in TNB (4.3 s) and slowest in FB (9.3 s).

3.3. Polymerization shrinkage stress

Representative curves for the polymerization shrinkage stress (MPa) of composites as a function of time (during 600 s) are shown in Fig.4a. An instantaneous increase in the shrinkage stress occurred during the initial 10 s of light-curing; thereafter, a slow increase was observed until the curing light was turned off. This was followed by a significant increase before a plateau was finally reached.

The maximum polymerization shrinkage stresses were, in decreasing order: Z350F 3.51 (0.30), TNB 2.42 (0.16), Z250 2.38 (0.33), SF 2.36 (0.18), FB 2.24 (0.13), and SDR 1.68 (0.18) (Fig. 4b). The lowest polymerization shrinkage stress was exhibited in SDR, while Z350F showed the highest polymerization shrinkage stress ($p < 0.05$). There were no statistical differences among TNB, Z250, SF, and FB ($p > 0.05$).

3.4. Acoustic emission during composite curing

The total AE events and amplitude distribution for 2,000 s after the initiation of light-curing

for each group are shown in Fig. 5a, and the total cumulative AE events as a function of time for each group are shown in Fig 5b. The mean numbers of AE events were, in decreasing order: Z350F 12.6 (1.34), TNB 7.0 (2.55), Z250 7.0 (1.22), FB 6.8 (1.79), SF 6.6 (1.82), and SDR 6.0 (1.58) (Fig. 5c). The highest AE event number was observed in Z350F ($p < 0.05$), while no statistical differences were found among the rest of the composites: TNB, Z250, FB, SF, and SDR ($p > 0.05$).

3.5. Relationship among the measured data

The correlation coefficients of the measured stress with shrinkage, modulus, and the product of shrinkage and modulus were, respectively, 0.49, 0.13, and 0.68. The measured stress correlated strongly with the number of AE events (r = 0.95).

4. Discussion

The present study measured the polymerization shrinkage, dynamic modulus, and shrinkage stress of six different composites in order to investigate the influence of two variables related to the properties of the composite material: the type (bulk-fill vs. conventional) and viscosity (non-flowable vs. flowable) of the composites.

Polymerization shrinkage has been reported to inversely correlate with the amount of filler.[1] In our study, the shrinkage strains of the flowable composites were higher than those of the non-flowable composites. Among the flowable composites, SDR showed the lowest shrinkage because it has a relatively high filler content compared to FB and Z350F. In addition, SDR contains a patented, modified UDMA (849 g/mol) that has a higher molecular weight than other monomers such as Bis-GMA (512 g/mol), Bis-EMA (496 g/mol), EPBADMA (452 g/mol), and conventional UDMA (470 g/mol). Shrinkage can be reduced by decreasing the number of reactive sites per unit volume via increasing the molecular weight of a monomer;[1,25] therefore, replacing conventional UDMA with the modified UDMA might be an additional contributing factor to the reduced shrinkage in SDR.

In spite of the similar filler contents in Z350F and FB, the lower shrinkage observed in

FB can be explained by the exclusion of the commonly added TEGDMA (286 g/mol), which has approximately half the molecular weight of the aforementioned dimethacrylates. However, the effect of monomer molecular weight on shrinkage could not be rationally evaluated between the composites because the proportion of each monomer present in the composites is not reported by the manufacturers.

Regarding the modulus development, higher modulus values were obtained in the non-flowable composites. This finding is in agreement with the generally reported observation that the modulus of composites, which is in direct contrast with the shrinkage strain, increases with increased filler content.[26-28] With the initiation of light-curing, the modulus of each material increased after a latent period of approximately 2 s in the non-flowable composites and 4 s in the flowable composites (Fig. 3a). This difference in latent period is related to the difference in the amount of filler incorporated into the composites. The lower filler content in the flowable composites appears to be responsible for the delayed modulus development (Fig. 3c).

For all of the composites, we observed two periods of time where the polymerization shrinkage stress rapidly increased. The first increase was observed during the initial 10 s of light-curing. This was followed by a rather slow increase until the curing light was turned off. This finding is consistent with the results of Al-Qudah et al.,[29] in that most of the polymerization reaction of a composite resin occurs immediately after light-curing. During

polymerization of a light-cured composite, the exothermic reaction of the composite and the radiant heat from the light-curing unit increase the temperature within the composite.[30] This causes a transient volumetric expansion of the composite, offsetting some of the developing shrinkage stress. The second marked increase in shrinkage stress was observed after the curing light was turned off and was attributed to the increase in composite shrinkage as a result of cooling.

Shrinkage stress can be directly influenced by instrument compliance. Min et al.[21] reported that the major factor controlling stress when instrument compliance was allowed without a feedback mechanism was shrinkage strain. Alternatively, the shrinkage strain and elastic modulus played comparable roles in the development of shrinkage stress when the compliance was restricted with a feedback mechanism. For stress measurement, we employed an instrument using a voice coil motor with a feedback mechanism in order to minimize instrument compliance.

The correlation coefficients of the measured stress with shrinkage ($r = 0.49$) and modulus ($r = 0.13$) were weak. On the other hand, the measured stress did positively correlate with the product of shrinkage and modulus at 20 s ($r = 0.68$).

The AE technique was used in this study to evaluate the debonding behavior of composites in human teeth. The quality of the bonded interface can also be assessed by confocal microscopy,[31] dye penetration,[32] micro-computed tomography (micro-CT),[33]

microtensile bond strength,[34] swept-source optical coherence tomography (SS-OCT),[35] and SEM.[36] However, these methods only provide post-evaluation of the interface after debonding has already occurred by polymerization shrinkage stress, and most of these methods require alteration of the test samples. In contrast, the AE technique enables non-destructive evaluation of debonding at the adhesive interface in real-time during composite curing. This is achieved by capturing elastic waves with an ultrasonic sensor as interfacial debonding occurs in the areas where the bond strength fails to withstand the shrinkage stress.[24]

Recent studies using this technique have confirmed that a slower rate of polymerization,[24] better bonding surface,[37,38] low-shrinkage composites,[24,39] and lower C-factor[38,40] are strongly associated with better resistance to interfacial debonding, as evidenced by fewer AE events. Previous studies evaluated the tooth-composite interface after AE examination by SEM[24,38] and micro-CT analysis,[39] where a positive association between AE events and interfacial debonding was found; wider and more micro-gaps were relatively frequently observed in specimens that had more AE events.

The shrinkage stress experienced by the composites was compared to the debonding behavior from the AE analysis in order to elucidate the relationship between them. A strong positive correlation ($r = 0.95$) was found between shrinkage stress and number of AE events, validating our second hypothesis. This finding corroborates previous studies that affirmed

the likelihood of interfacial debonding with increasing shrinkage stress.[24,37-40]

The non-flowable composites exhibited similar AE event numbers, for both bulk-fill (TNB and SF) and conventional composites (Z250). In contrast, different shrinkage stress values and AE events were observed among the flowable composites. The bulk-fill flowable composites (FB and SDR) showed much better results than the conventional flowable (Z350F) composite; this could be explained by their lower shrinkage and modulus values. Among the bulk-fill composites, there were no significant differences in shrinkage stress or AE events, except for one of the flowable composites (SDR), which generated a significantly lower shrinkage stress. Therefore, the first hypothesis of this study, stating that bulk-fill and conventional composites would not exhibit different polymerization characteristics, was partially supported.

In the present study, a single type of adhesive system (Adper Scotchbond Multi-Purpose) was used in order to facilitate standardized conditions, thereby allowing us to focus on the variables related to the material. Discrepant results might be observed if each composite was bonded with the corresponding adhesive system recommended by the manufacturers. However, the rationale for the use of a single adhesive system is based on the principle of resin bonding where the methacrylate group of the adhesive cross-links with the resin matrix of the composites.

Within the limitations of this study, considering the similar results between the non-

flowable composites, bulk filling of the non-flowable bulk-fill composites is not necessarily recommended over incremental layering of the conventional composite. In contrast, compared with the flowable conventional composite, the flowable bulk-fill composites showed better performance in terms of shrinkage stress and debonding behavior. Therefore, provided that flowable bulk-fill composites have the mechanical properties required to replace dentin for clinical function, the flowable bulk-fill composites (especially SDR) may be suitable for the core build-up of endodontically treated teeth or for filling deep cavities, assuming a 2-mm occlusal space is left for subsequent capping with a conventional non-flowable composite. Although occlusal capping requires an additional procedure, decreasing the convenience of the bulk-fill composites, the use of flowable bulk-fill composites is still time-saving for dentists compared to the use of conventional composites that require incremental layering and curing processes. Furthermore, clinicians would not need to worry about contamination or void formation, which can occur with the inadvertent placement of non-flowable composites between increments or at the tooth-composite interface, due to the relative difficulty in adaptation.

Despite the benefits, the use of the bulk-fill composites has to be judiciously made. As compared to the non-flowable composites, the flowable bulk-fill composites tend to absorb more moisture,[41] compromising the property of the material and the integrity of the bonding interface. Thus, an outer capping layer with a non-flowable composite over the flowable

composite is recommended not only in occlusal load-bearing area but also in all situations where direct exposure of the material to the oral fluid is anticipated. Therefore, it is important to note that the flowable bulk-fill composites should not be used to substitute the enamel; the flowable composites needs to be cautiously applied when the cavity has missing axial wall such as in Class II restorations because the material is likely to flow onto the outer cavity surface. Clinicians should keep in mind that bulk-fill composites cannot entirely replace conventional composites, and that the incremental technique is preferred over the bulk filling technique in order to minimize polymerization shrinkage stress, irrespective of the type of composite.

5. Conclusions

There were significant differences in the polymerization shrinkage, dynamic modulus development, and shrinkage stress among the composites. AE analysis confirmed a strong linear relationship between shrinkage stress and debonding at the tooth-composite interface. In terms of polymerization shrinkage stress and tooth-composite interfacial debonding behavior, the non-flowable bulk-fill composites (TNB and SF) do not seem to be advantageous compared to the non-flowable conventional composite (Z250), while the flowable bulk-fill composites (FB and SDR) demonstrated superior results compared with the flowable conventional composite (Z350F).

6. References

[1] Braga RR, Ballester RY, Ferracane JL. Factors involved in the development of polymerization shrinkage stress in resin-composites: a systematic review. *Dental Materials* 2005;21:962-70.

[2] Ellakwa A, Cho N, Lee IB. The effect of resin matrix composition on the polymerization shrinkage and rheological properties of experimental dental composites. *Dental Materials* 2007;23:1229-35.

[3] Kleverlaan CJ, Feilzer AJ. Polymerization shrinkage and contraction stress of dental resin composites. *Dental Materials* 2005;21:1150-7.

[4] Lee IB, Cho BH, Son HH, Um CM. A new method to measure the polymerization shrinkage kinetics of light cured composites. *Journal of Oral Rehabilitation* 2005;32:304-14.

[5] Ferracane JL. Developing a more complete understanding of stresses produced in dental composites during polymerization. *Dental Materials* 2005;21:36-42.

[6] Kwon Y, Ferracane J, Lee IB. Effect of layering methods, composite type, and flowable liner on the polymerization shrinkage stress of light cured composites. *Dental Materials* 2012;28:801-9.

[7] Park J, Chang J, Ferracane J, Lee IB. How should composite be layered to reduce shrinkage stress: incremental or bulk filling? *Dental Materials* 2008;24:1501-5.

[8] Feilzer AJ, De Gee AJ, Davidson CL. Setting stress in composite resin in relation to configuration of the restoration. *Journal of Dental Research* 1987;66:1636-9.

[9] Bucuta S, Ilie N. Light transmittance and micro-mechanical properties of bulk fill vs. conventional resin based composites. *Clinical Oral Investigations* 2014;18:1991-2000.

[10] Ilie N, Bucuta S, Draenert M. Bulk-fill resin-based composites: an in vitro assessment of their mechanical performance. *Operative Dentistry* 2013;38:618-25.

[11] Ilie N, Schoner C, Bucher K, Hickel R. An in-vitro assessment of the shear bond strength of bulk-fill resin composites to permanent and deciduous teeth. *Journal of Dentistry* 2014;42:850-5.

[12] Moorthy A, Hogg CH, Dowling AH, Grufferty BF, Benetti AR, Fleming GJ. Cuspal deflection and microleakage in premolar teeth restored with bulk-fill flowable resin-based composite base materials. *Journal of Dentistry* 2012;40:500-5.

[13] Leprince JG, Palin WM, Vanacker J, Sabbagh J, Devaux J, Leloup G. Physico-mechanical characteristics of commercially available bulk-fill composites. *Journal of Dentistry* 2014;42:993-1000.

[14] Alshali RZ, Silikas N, Satterthwaite JD. Degree of conversion of bulk-fill compared to conventional resin-composites at two time intervals. *Dental Materials*

2013;29:e213-7.

[15] Flury S, Hayoz S, Peutzfeldt A, Husler J, Lussi A. Depth of cure of resin composites: is the ISO 4049 method suitable for bulk fill materials? *Dental Materials* 2012;28:521-8.

[16] Garcia D, Yaman P, Dennison J, Neiva G. Polymerization Shrinkage and Depth of Cure of Bulk Fill Flowable Composite Resins. *Operative Dentistry* 2013;39:441-8.

[17] Ilie N, Kessler A, Durner J. Influence of various irradiation processes on the mechanical properties and polymerisation kinetics of bulk-fill resin based composites. *Journal of Dentistry* 2013;41:695-702.

[18] Furness A, Tadros MY, Looney SW, Rueggeberg FA. Effect of bulk/incremental fill on internal gap formation of bulk-fill composites. *Journal of Dentistry* 2014;42:439-49.

[19] El-Safty S, Silikas N, Watts DC. Creep deformation of restorative resin-composites intended for bulk-fill placement. *Dental Materials* 2012;28:928-35.

[20] El-Damanhoury H, Platt J. Polymerization shrinkage stress kinetics and related properties of bulk-fill resin composites. *Operative Dentistry* 2014;39:374-82.

[21] Min SH, Ferracane J, Lee IB. Effect of shrinkage strain, modulus, and instrument compliance on polymerization shrinkage stress of light-cured composites during the initial curing stage. *Dental Materials* 2010;26:1024-33.

[22] Lee IB, Cho BH, Son HH, Um CM, Lim BS. The effect of consistency, specimen geometry and adhesion on the axial polymerization shrinkage measurement of light cured composites. *Dental Materials* 2006;22:1071-9.

[23] Kim MH, Min SH, Ferracane J, Lee IB. Initial dynamic viscoelasticity change of composites during light curing. *Dental Materials* 2010;26:463-70.

[24] Cho NY, Ferracane JL, Lee IB. Acoustic emission analysis of tooth-composite interfacial debonding. *Journal of Dental Research* 2013;92:76-81.

[25] Cramer NB, Stansbury JW, Bowman CN. Recent advances and developments in composite dental restorative materials. *Journal of Dental Research* 2011;90:402-16.

[26] Masouras K, Silikas N, Watts DC. Correlation of filler content and elastic properties of resin-composites. *Dental Materials* 2008;24:932-39.

[27] Davidson CL, Feilzer AJ. Polymerization shrinkage and polymerization shrinkage stress in polymer-based restoratives. *Journal of Dentistry* 1997;25:435-40.

[28] Lee JH, Um CM, Lee IB. Rheological properties of resin composites according to variations in monomer and filler composition. *Dental Materials* 2006;22:515-26.

[29] Al-Qudah AA, Mitchell CA, Biagioni PA, Hussey DL. Thermographic investigation of contemporary resin-containing dental materials. *Journal of Dentistry* 2005;33:593-602.

[30] Lloyd CH, Joshi A, McGlynn E. Temperature rises produced by light sources and

composites during curing. *Dental Materials* 1986;2:170-4.

[31] Sauro S, Mannocci F, Toledano M, Osorio R, Thompson I, Watson TF. Influence of the hydrostatic pulpal pressure on droplets formation in current etch-and-rinse and self-etch adhesives: a video rate/TSM microscopy and fluid filtration study. *Dental Materials* 2009;25:1392-402.

[32] Leevailoj C, Cochran MA, Matis BA, Moore BK, Platt JA. Microleakage of posterior packable resin composites with and without flowable liners. *Operative Dentistry* 2001;26:302-7.

[33] De Santis R, Mollica F, Prisco D, Rengo S, Ambrosio L, Nicolais L. A 3D analysis of mechanically stressed dentin-adhesive-composite interfaces using X-ray micro-CT. *Biomaterials* 2005;26:257-70.

[34] Takemori T, Chigira H, Itoh K, Hisamitsu H, Wakumoto S. Factors affecting tensile bond strength of composite to dentin. *Dental Materials* 1993;9:136-8.

[35] Nazari A, Sadr A, Shimada Y, Tagami J, Sumi Y. 3D assessment of void and gap formation in flowable resin composites using optical coherence tomography. *Journal of Adhesive Dentistry* 2013;15:237-43.

[36] Ciucchi B, Bouillaguet S, Delaloye M, Holz J. Volume of the internal gap formed under composite restorations in vitro. *Journal of Dentistry* 1997;25:305-12.

[37] Gu JU, Choi NS. Evaluation of marginal failures of dental composite restorations by

acoustic emission analysis. *Dental Materials Journal* 2013;32:398-404.

[38] Kim RJ, Choi NS, Ferracane J, Lee IB. Acoustic emission analysis of the effect of simulated pulpal pressure and cavity type on the tooth-composite interfacial de-bonding. *Dental Materials* 2014;30:876-83.

[39] Li H, Li J, Yun X, Liu X, Fok AS. Non-destructive examination of interfacial debonding using acoustic emission. *Dental Materials* 2011;27:964-71.

[40] Liu X, Li H, Li J, Lu P, Fok AS. An acoustic emission study on interfacial debonding in composite restorations. *Dental Materials* 2011;27:934-41.

[41] Jang JH, Park SH, Hwang IN. Polymerization Shrinkage and Depth of Cure of Bulk-Fill Resin Composites and Highly Filled Flowable Resin [published online ahead of print August 19, 2014]. *Operative Dentistry* doi: 10.2341/13-307-L.

Table and Figures

Table 1. Composite materials used in this study

Materials (Code, shade, lot No.)	Type	Composition	Manufacturer
Filtek Z250 (Z250, A2, N482264)	C, NF	Bis-GMA, Bis-EMA, TEGDMA, UDMA, zirconia, silica (82 wt% / 60 vol%)	3M ESPE, St. Paul, MN, USA
SonicFill (SF, A2, 5026722)	B, NF	Bis-GMA, TEGDMA, EBPDMA, silica, glass, oxide (83.5 wt% / 69 vol%)	Kerr, Orange, CA, USA
Tetric N-Ceram Bulk Fill (TNB, IVA, S09719)	B, NF	Dimethacrylates, polymer filler, barium glass, ytterbium trifluoride, mixed oxide (78 wt% / -)	Ivoclar Vivadent, Schaan, Liechtenstein
Filtek Z350 XT Flowable (Z350F, A2, N50234)	C, F	Bis-GMA, Bis-EMA, TEGDMA, zirconia, silica (65 wt% / -)	3M ESPE, St. Paul, MN, USA
SureFil SDR Flow (SDR, A2, 130630)	B, F*	SDR patented UDMA, TEGDMA, EBPDMA, barium and strontium alumino-fluoro-silicate glass (68 wt% / 45 vol%)	Dentsply, Konstanz, Germany
Filtek Bulk Fill (FB, A2, N540884)	B, F*	Bis-GMA, UDMA, Bis-EMA(6), procrylat resins, ytterbium trifluoride, zirconia, silica (64.5 wt% / 42.5 vol%)	3M ESPE, St. Paul, MN, USA

Abbreviations: B, bulk-fill; C, conventional; NF, non-flowable; F, flowable. *, bulk-fill composites requiring a 2-mm capping layer as recommended by manufacturers. Bis-EMA, bisphenol-A polyethylene glycol diether dimethacrylate; Bis-GMA, bisphenol-A diglycidyl ether dimethacrylate; EBPDMA, ethoxylated bisphenol-A-dimethacrylate; TEGDMA, triethylene glycol dimethacrylate; UDMA, urethane dimethacrylate.

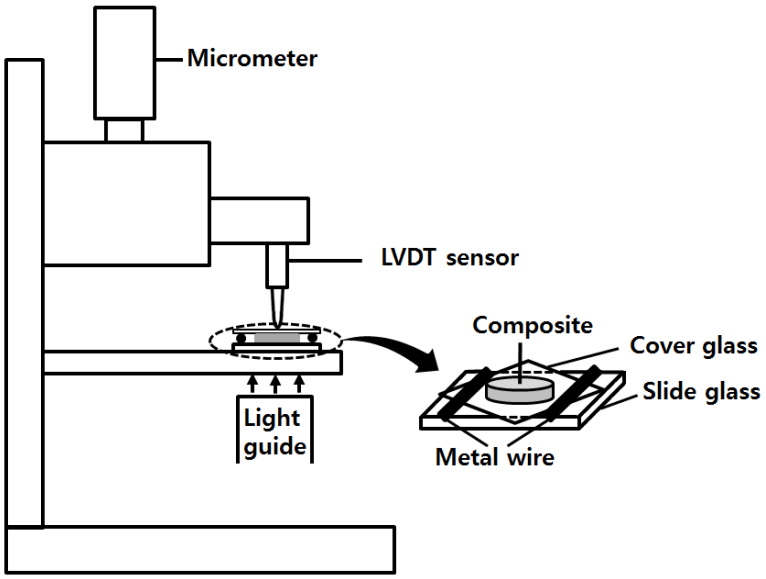
Micrometer
LVDT sensor
Composite
Cover glass
Slide glass
Light guide
Metal wire

(a)

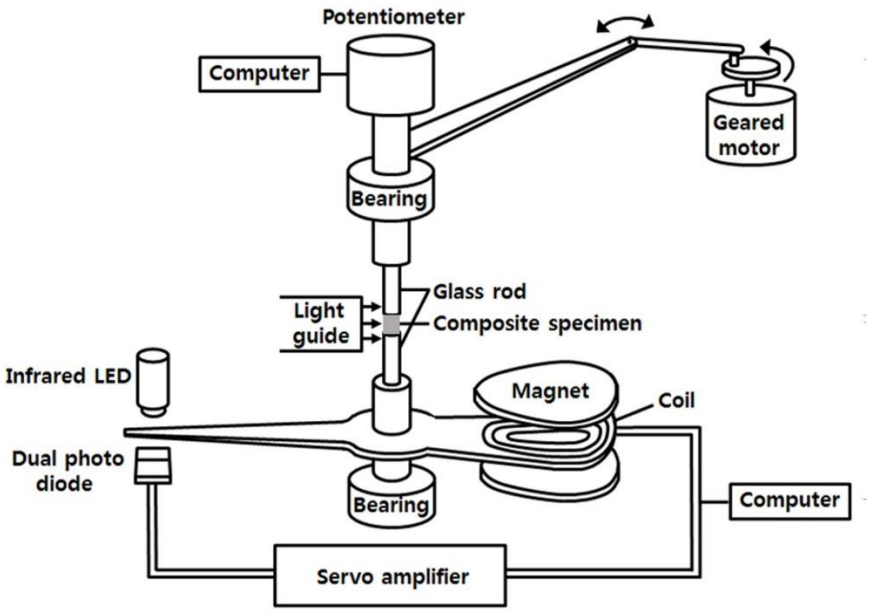
Potentiometer
Computer
Geared motor
Bearing
Glass rod
Light guide
Composite specimen
Infrared LED
Magnet
Coil
Dual photo diode
Bearing
Computer
Servo amplifier

(b)

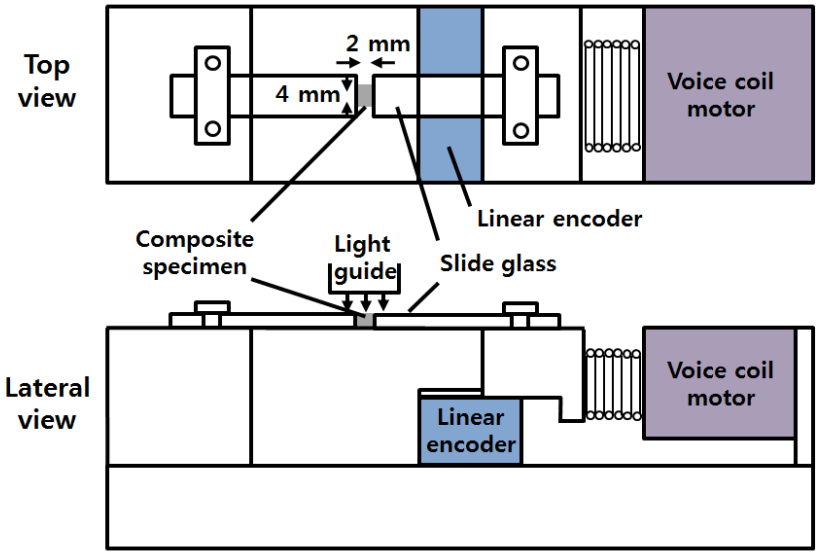

(c)

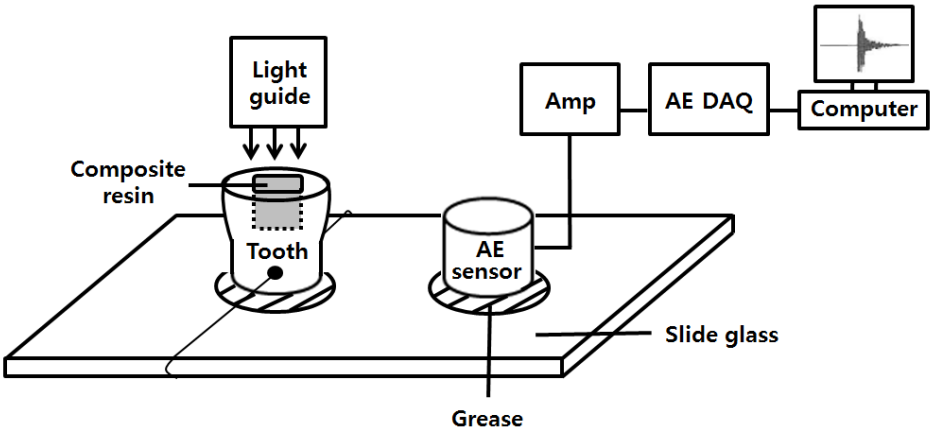

(d)

Figure 1. Schematic diagram of the instrument for (a) axial shrinkage measurement, (b) dynamic modulus measurement, (c) polymerization shrinkage stress measurement, and (d) AE analysis of debonding behavior at the tooth-composite interface.

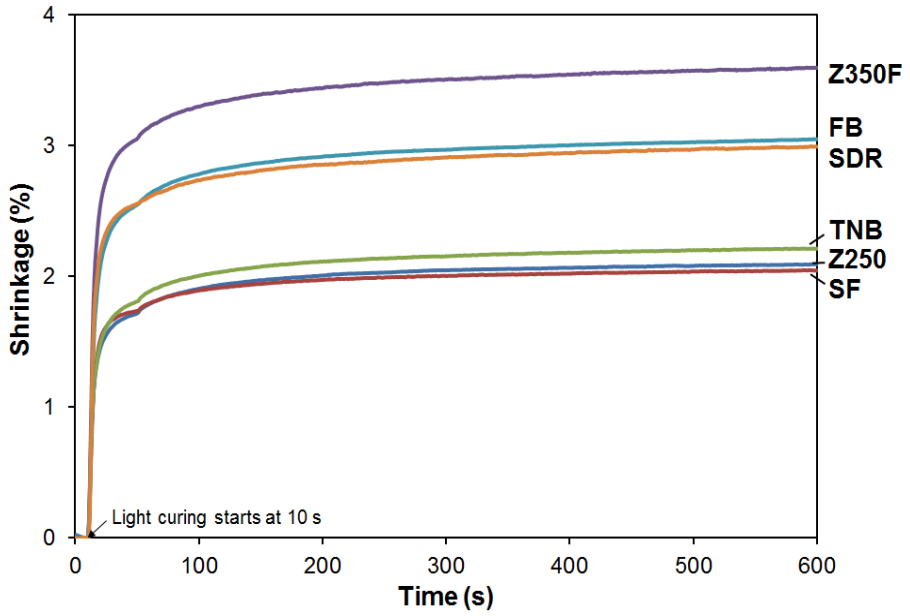

(a)

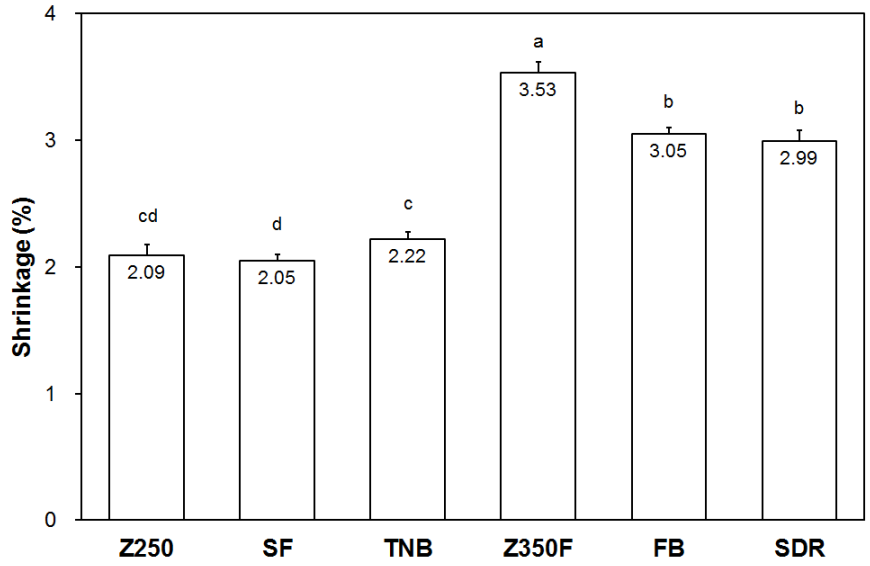

(b)

Figure 2. (a) Shrinkage (%) as a function of time, and (b) shrinkage at 600 s.

The same lower case letters indicate that there is no statistical difference ($p > 0.05$).

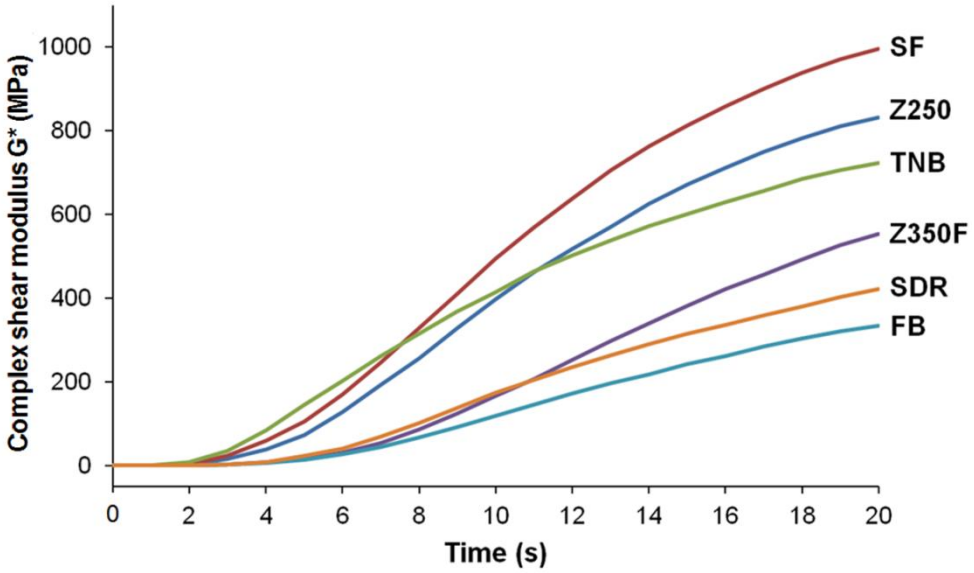
Complex shear modulus G* (MPa)
1000
800
600
400
200
0
0
2
4
6
8
10
12
14
16
18
20
Time (s)
SF
Z250
TNB
Z350F
SDR
FB

(a)

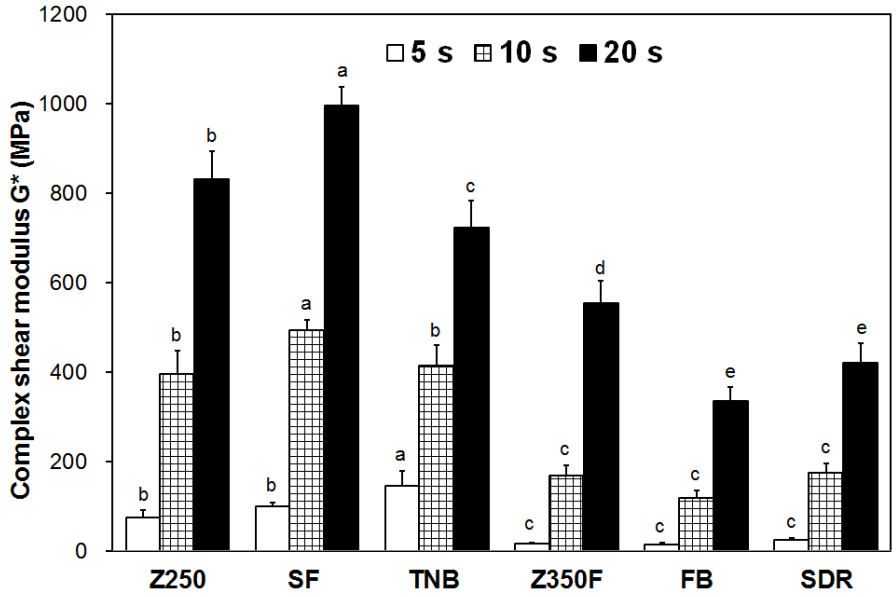
Complex shear modulus G* (MPa)
1200
1000
800
600
400
200
0
5 s
10 s
20 s
Z250
SF
TNB
Z350F
FB
SDR

(b)

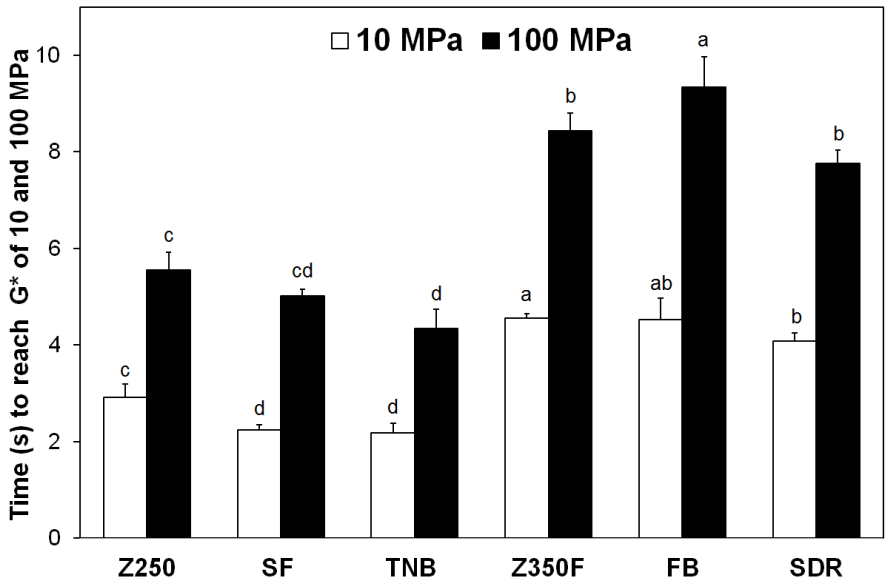

(c)

Figure 3. (a) Development of complex shear modulus (MPa) as a function of time. (b) Complex shear modulus at curing time of 5 s, 10 s, and 20 s. (c) Time (s) to reach a complex shear modulus of 10 and 100 MPa.

Values with the same lower case letters are not significantly different among the materials ($p > 0.05$).

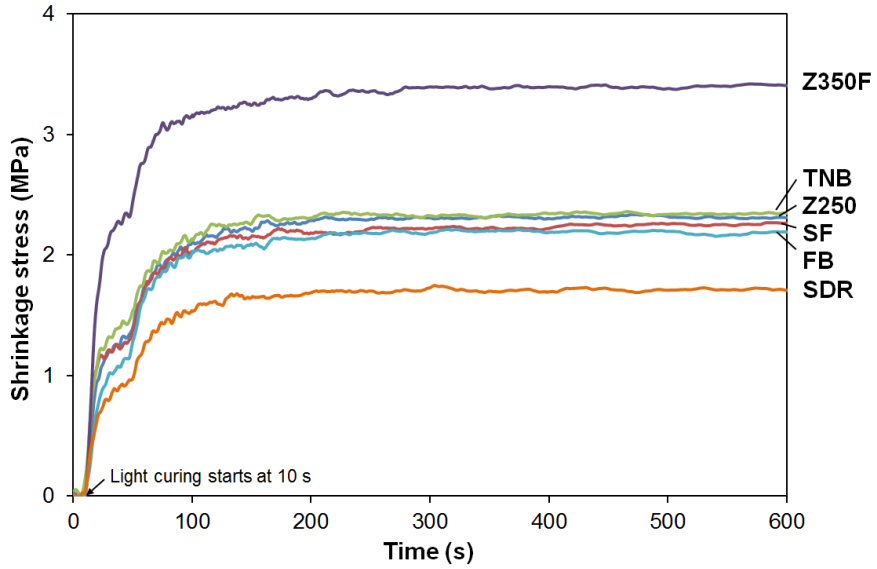

(a)

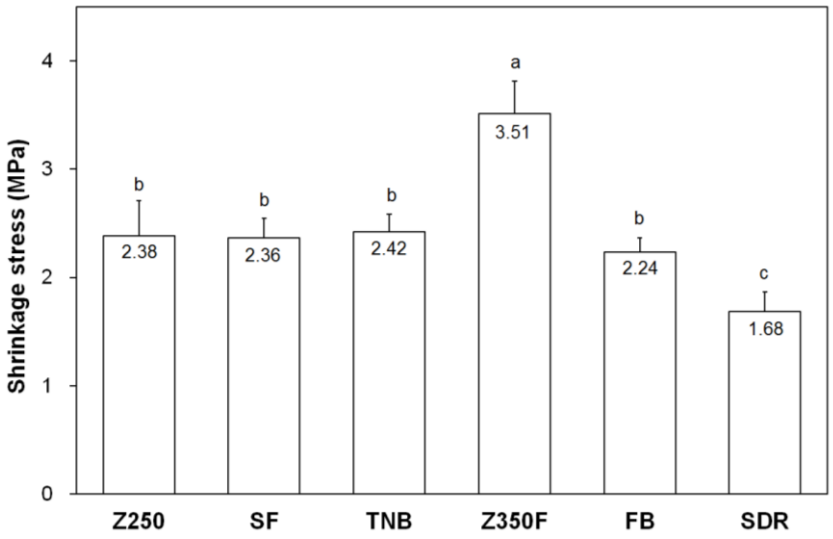

(b)

Figure 4. (a) Representative curves of polymerization shrinkage stress (MPa). (b) Shrinkage stress at 600 s.

The same lower case letters indicate that there is no statistical difference ($p > 0.05$).

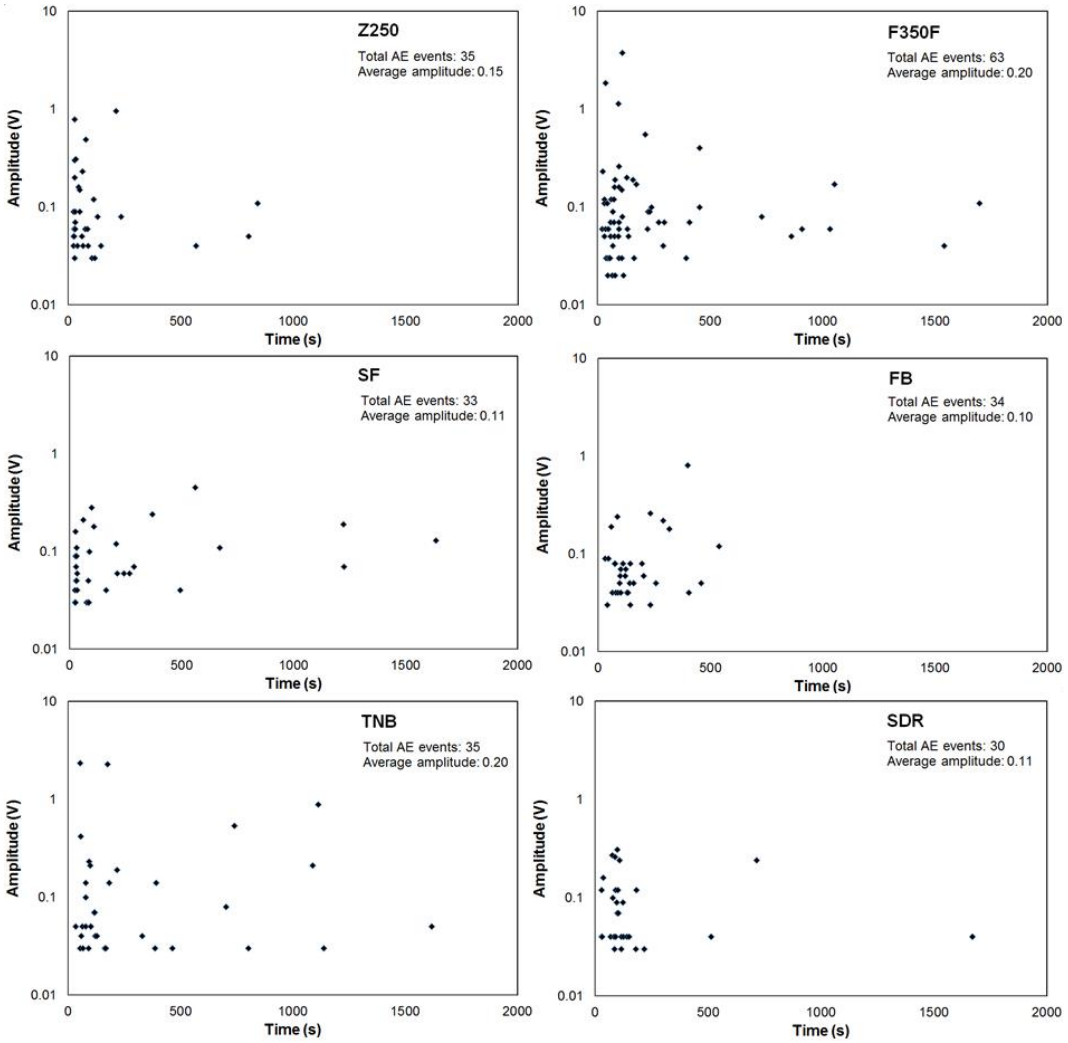
Z250
Total AE events: 35
Average amplitude: 0.15
F350F
Total AE events: 63
Average amplitude: 0.20
SF
Total AE events: 33
Average amplitude: 0.11
FB
Total AE events: 34
Average amplitude: 0.10
TNB
Total AE events: 35
Average amplitude: 0.20
SDR
Total AE events: 30
Average amplitude: 0.11
Amplitude (V)
Time (s)
10
1
0.1
0.01
0
500
1000
1500
2000

(a)

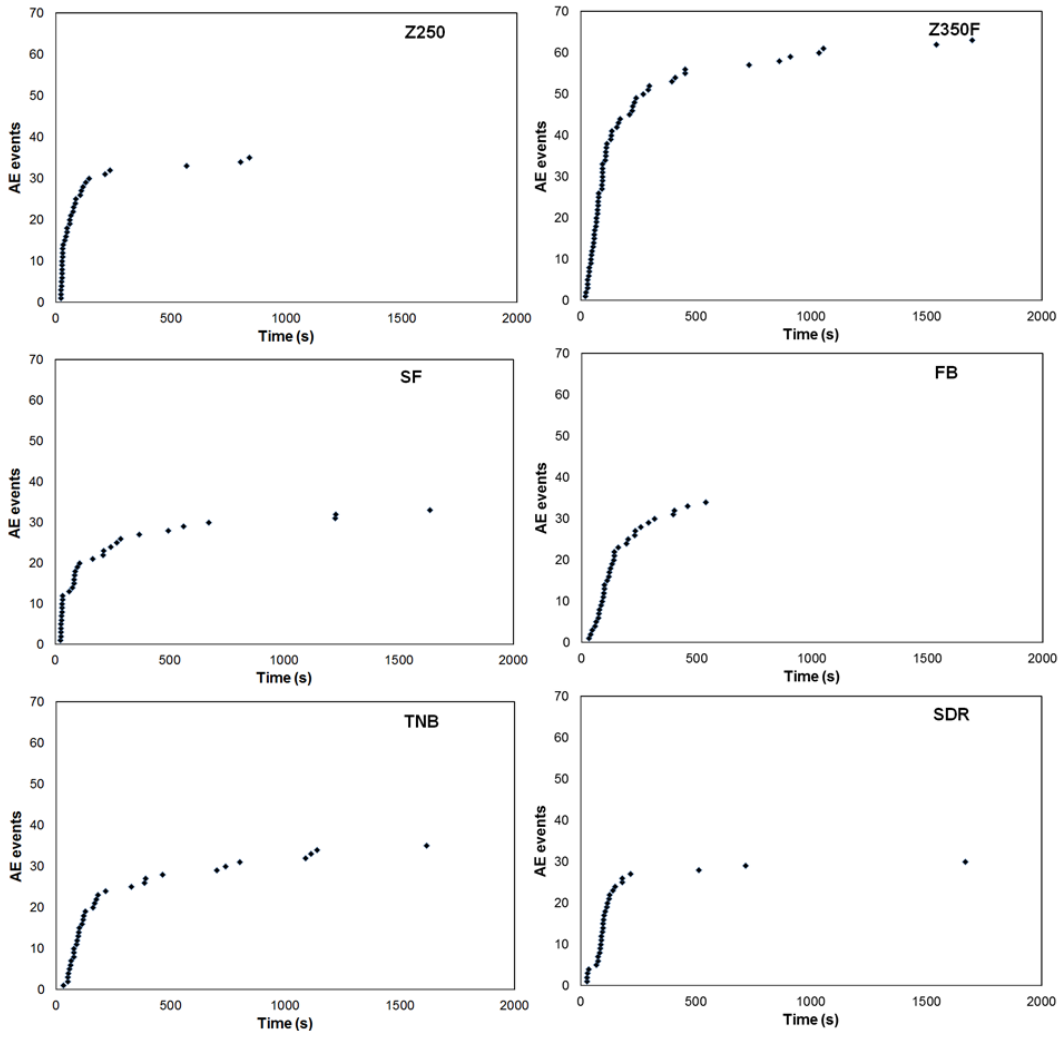
Z250
Z350F
SF
FB
TNB
SDR
AE events
Time (s)
0
10
20
30
40
50
60
70
500
1000
1500
2000

(b)

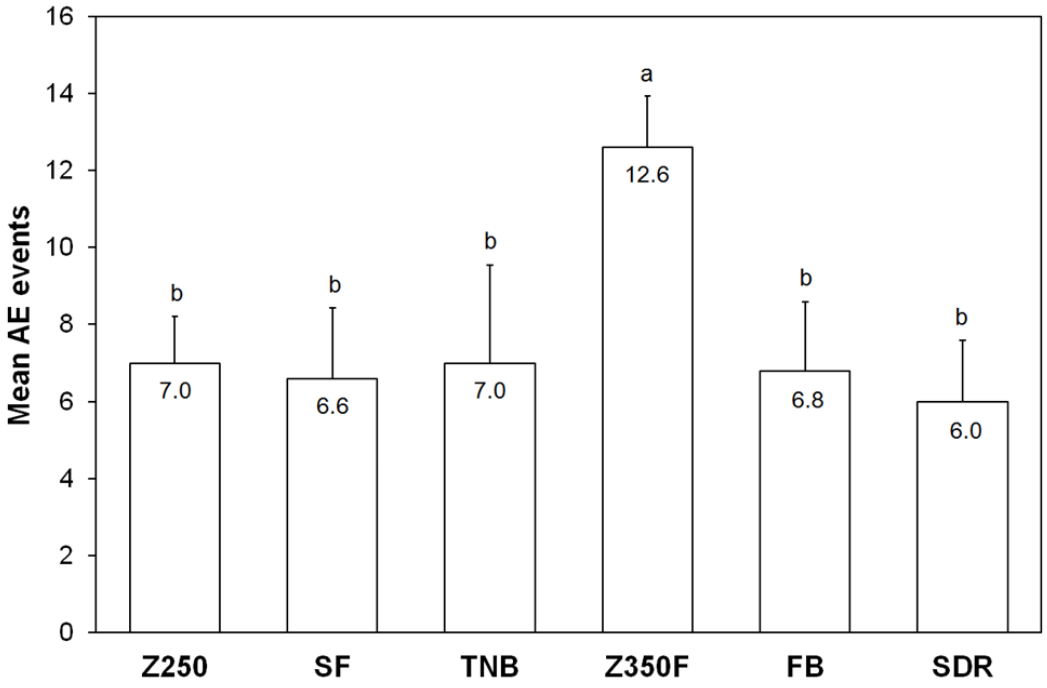

(c)

Figure 5. (a) Total AE events and amplitude distribution. (b) Cumulative AE events as a function of time. (c) Mean number of AE events of each composite.

The same lower case letters indicate that there is no statistical difference ($p > 0.05$).

국문초록

Bulk-fill 복합레진 수복시 치아-수복물 계면 파괴와 관련된 중합수축, 탄성계수, 수축응력

김 진 영

서울대학교 대학원 치의과학과 치과보존학 전공

(지도교수 이 인 복)

1. 목적

본 연구의 목적은 bulk-fill 복합레진과 conventional 복합레진의 중합수축, 탄성계수, 중합수축응력을 측정하여 비교하고, 중합수축응력과 치아-레진 계면 파괴와의 연관성을 알아보기 위함이다.

2. 재료 및 방법

2 종의 non-flowable bulk-fill: SonicFill (SF)과 Tetric N-Ceram Bulk Fill (TNB), 2 종의 flowable bulk-fill: Filtek Bulk Fill (FB)과 SureFil SDR Flow (SDR, Dentsply), 1 종의 non-flowable conventional 복합레진: Filtek Z250 (Z250, 3M ESPE), 1 종의 flowable conventional 복합레진: Filtek Z350 XT Flowable (Z350F, 3M ESPE)을 사용하여 중합 시 발생하는 수축량, 동적 탄성계수, 수축응력을 자체 제작한 장비를 이용하여 측정하였다(n = 5). 복합레진 수복 시 발생하는 치아-레진 계면 파괴를 알아보기 위해 건전한 대구치에 1급 와동을 형성하고 각 복합레진으로 충전한 후 음향방출 시험을 시행하였다(n = 5).

3. 결과

중합수축(%)은 Z350F (3.53)에서 가장 높게 측정되었고, FB (3.05), SDR (2.99), TNB (2.22), Z250 (2.09), SF (2.05) 순으로 감소하였다. 복소전단탄성계수(MPa)는 SF (996.2), Z250 (831.8), TNB (723.6), Z350F (553.2), SDR (421.3), FB (334.8) 순으로 감소하였다. 중합수축응력(MPa)은 Z350F (3.51), TNB (2.42), Z250 (2.38), SF (2.36), FB (2.24), SDR (1.68)였다. 음향방출 사상수는 Z350F (12.6), TNB (7.0), Z250 (7.0), FB (6.8), SF (6.6), SDR (6.0)였다. Z350F 에서 가장 높은 중합수축응력과 가장 많은 음향방출 사상수가 측정되었고, SDR 에서 가장 낮은 중합수축응력이 관찰되었다 ($p < 0.05$). TNB, Z250, SF, FB 의 중합수축응력과 TNB, Z250,

FB, SF, SDR 의 음향방출 사상수에서는 유의한 차이를 보이지 않았다 ($p > 0.05$).

4. 결론

음향방출시험을 통해 치아-레진 계면부의 접착파괴와 중합수축응력 사이에 강한 상관관계를 확인하였다. 중합수축응력 및 치아-복합레진 계면 파괴는 non-flowable 복합레진(bulk-fill 복합레진과 conventional 복합레진)간에 차이가 없었으나, flowable 복합레진에서는 bulk-fill 복합레진이 conventional 복합레진 보다 중합수축응력이 낮았고 치아-복합레진 계면 파괴가 적게 나타났다.

주요어: 음향방출시험, bulk-fill 복합레진, 탄성계수, 중합수축, 중합수축응력

학 번: 2012-31170